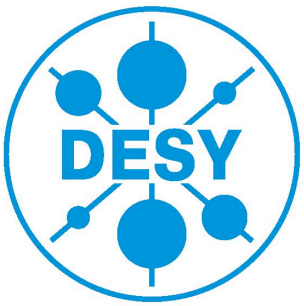

Analysis of Pedestal Data of The Alibava Readout System

Sergi Navarro, University of Valencia, Spain

Supervised by Eda Yildirim, DESY ATLAS Group

September 11, 2014

Abstract

One of the projects in ATLAS group of DESY is to measure Lorentz angle on highly irradiated ATLAS silicon strip sensors. The Alibava readout system is used to read the signal of the sensors. Its pedestal and noise signal are studied in this summer student project. The work summarised here consists of the analysis of the dependence of pedestal and noise on temperature and magnetic field for non-irradiated, irradiated and annealed samples.

Contents

1 Introduction

The work done by Glashow, Weinberg and Salam on the unification of electromagnetic and weak interactions, together with the discovery of new subatomic particles, led naturally to the Standard Model in the mid-1970s. Since then, discoveries of the top quark (1995), the tau neutrino (2000), and Higgs boson (2013), have given further credence to it [1]. Despite all its successes, there remain some puzzling aspects of the Standard Model of two categories: intrinsic aspects such as the hierarchy problem or the existence of supersymmetric particles and the extrinsic problem of not being able to account for gravitation. Experiments have been proposed to solve these problems. For example the searching for super symmetric particles is one of the most important aims of particle physics and the Large Hadron Collider (LHC) will play an important role on it. In order to further increase its discovery potential beyond 2020, LHC needs an upgrade to increase the total number of collisions by a factor of 10. The new High-Luminosity LHC (HL-LHC) will provide more accurate measurements and enable observation of not previously witnessed processes that occur below the current sensitivity level. At this point one can clearly see the necessity of developing new detectors capable of providing us with new observations. This will ultimately allow us to discern among the proposed theories that make different predictions.

This report constitutes a summary of a summer student project about a particular analysis proposed by my supervisor Eda Yildirim: The analysis of pedestal and noise signal on the Alibava readout system for the Lorentz angle experiment. In the first part we have reviewed the main ingredients of particle detectors in the reconstruction of particle tracks. Later, we have focussed attention in the Lorentz angle measurement for our strip silicon sensor, including a short description of the experiment setup and the Alibava readout system. During the experiment pedestal and noise data was collected. In the analysis part we present the results of the pedestal and noise analysis of the Alibava readout system.

1.1 The ATLAS Inner Detector

The ATLAS detector [2] is the largest High Energy Physics detector constructed so far. It is a toroidal detector at the LHC at CERN. It consists of a series of ever-larger concentric cylinders around the interaction point where the proton beams from the LHC collide. It can be divided into four major parts: the inner detector, the calorimeters, the muon spectrometer and the magnet systems.
The inner detector [3] shown in Figure (1) is the first cylindrical volume of the detector that the particles traverse. The charged particles that come out from the collision fly through subsequent detectors, generating a wake of points corresponding to the fired sensors. Thus one can reconstruct the particle trajectory, and from there, derive the nature and properties of these particles. For instance the degree of curvature reveals the momentum of the particles and one can also know the particle charge by looking at the

direction of the curve.

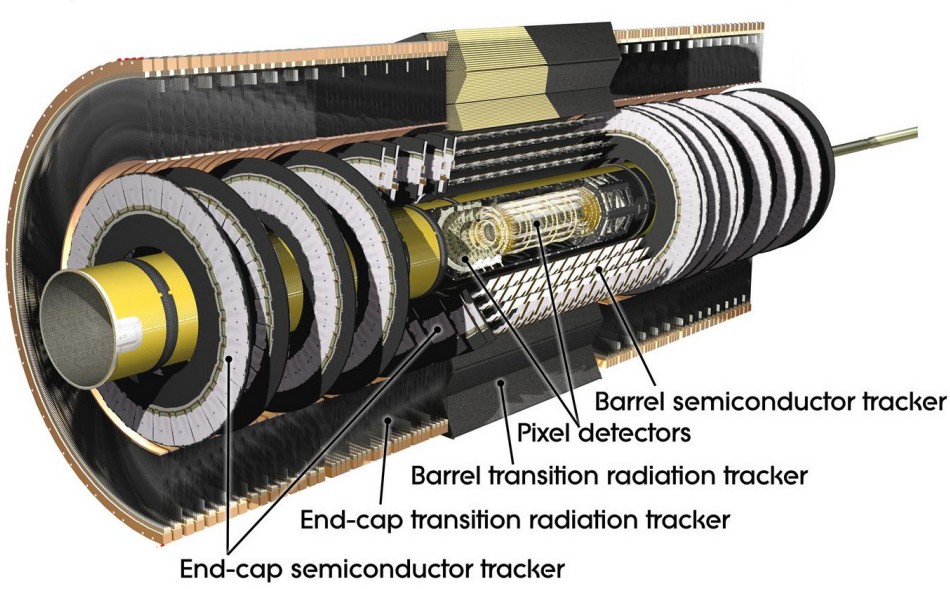

Figure 1: Current ATLAS inner detector.

1.2 ATLAS Semiconductor Tracker for HL-LHC

The current inner detector was designed to operate for 10 years at a peak luminosity of 10^{23} $\mathrm{cm}^{-2}\mathrm{s}^{-1}$. With the HL-LHC the luminosity will increase to up to 10^{35} $\mathrm{cm}^{-2}\mathrm{s}^{-1}$. Increasing the luminosity will cause an increase in radiation damage. The current semiconductor tracker can operate up to a fluence of $2 \times 10^{14}(1MeVn_{eq})/\mathrm{cm}^2$ which is significantly lower than the $\sim 10^{15}(1MeVn_{eq})/\mathrm{cm}^2$ expected at the HL-LHC [4], see Figure(2). It is important to study the properties of silicon sensors before and after irradiation because the detector material is damaged under impact of radiation. For instance the Lorentz angle in silicon sensors will be affected. One of the future goals of this project is to analyse this change. The Lorentz angle, and how we measure it, will be explained in the following sections.

How Radiation affects the sensors?

The structure of the atomic lattice within the sensor material is damaged when the sensor is exposed to radiation. Different particle types with different energies affect the distribution of the defects in the lattice in different ways. As defects are introduced to the silicon, additional energy levels in between the valence band and the conduction band are created. This levels can act as additional donors or acceptors and change the effective doping. As the depletion voltage depends on the doping concentration in the

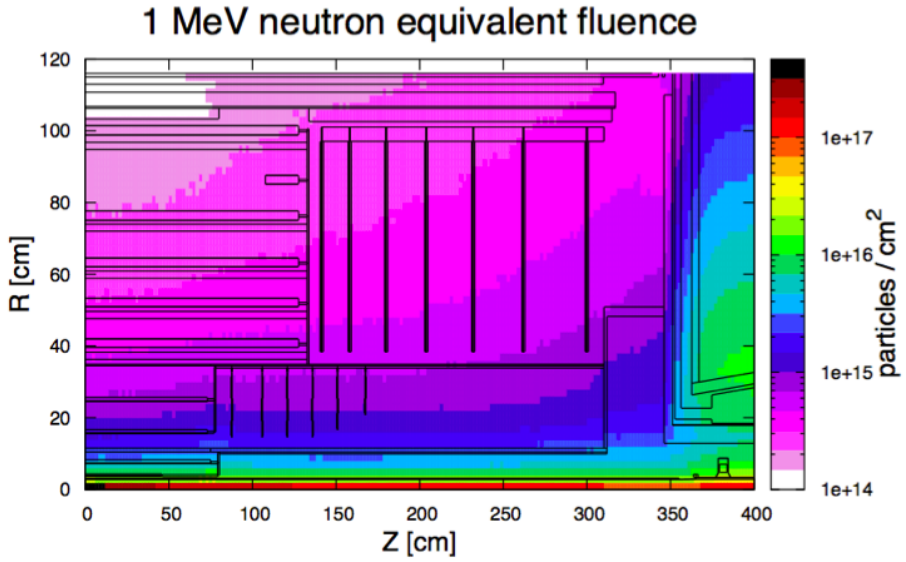

Figure 2: Background Radiation Simulation. *RZ*-map of the 1MeV neutron equivalent fluence in the Inner Tracker region, normalised to 3000 fb^{-1} of 14 TeV minimum bias events generated unit PYTHIA8 [4].

sensor, the current and voltage properties are also affected. Intermediate states within the band gap can also enhance the level of leakage current. Another phenomena arises when the additional energy levels create a potential well, where the electrons are trapped in a bound state. If the time during which the electron is captured in the well exceeds the readout time, then its charge is lost for the signal generation [5].

2 The Lorentz Angle Measurement

2.1 Theory

When an ionised particle passes through a semiconductor material, it produces free electrons and holes. As a result a number of electrons are transferred from the valence band to the conduction band while the valence band is filled with the same number of holes. If this happens in a region of the space under the influence of an electric field, the electrons are driven towards the electrodes, opposite to the direction of the field. In this way they generate a pulse that can be measured in an external circuit. Figure (3) shows an schematic picture of this mechanism.
In the ATLAS experiment, the detectors are exposed to a magnetic field up to 2 Tesla. When we have a magnetic field the situation slightly changes. In this case the electrons experience a Lorentz force that (as a good approximation) deflects them with respect to

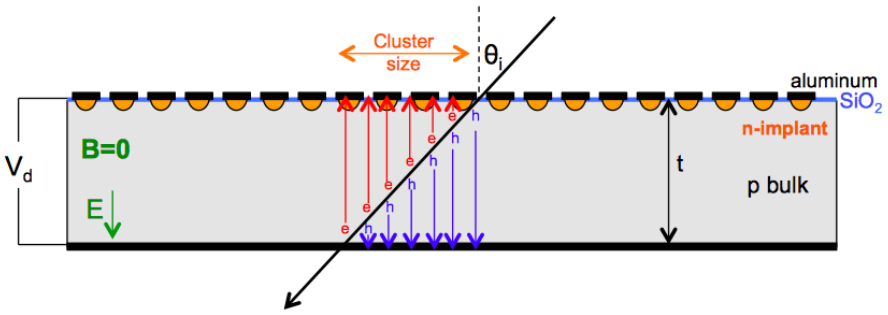

Figure 3: Schematic view of a charged particle traversing the sensor with incident angle θ_i under zero magnetic field.

the direction of the electric field by an angle that can be calculated from the formula [6]

$$\tan\theta_L \simeq \frac{F_{\vec{B}}}{F_{\vec{E}}} \simeq \frac{v_s B}{E} = \mu_H B = r\mu_d B \tag{1}$$

This is the so called Lorentz Angle, where μ_H is the Hall mobility, μ_d is the drif mobility, and r is the Hall factor that depends on the details of the scattering mechanism of charge carriers in the material. For silicon the following parametrization can be adopted

$$\mu_d = \frac{v_s/E_c}{[1+(E/E_c)^\beta]^{1/\beta}} \tag{2}$$

	Electrons	Holes
$v_s(\text{cm s}^{-1})$	$1.53 \cdot 10^9 \cdot T^{-0.87}$	$1.62 \cdot 10^8 \cdot T^{-0.52}$
$E_c(\text{V cm}^{-1})$	$1.01 \cdot T^{1.55}$	$1.24 \cdot T^{1.68}$
β	$2.57 \cdot 10^{-2} \cdot T^{0.66}$	$0.46 \cdot T^{0.17}$
r	$1.13 + 0.0008 \cdot (T - 273)$	$0.72 - 0.0005 \cdot (T - 273)$

Figure 4: Temperature dependence of the parameters for silicon.

All the parameters are defined in Figure (4), where v_s is the drift velocity, E_c is the critical electric field, β is a parameter that depends on the temperature T and E is the electric field.

2.2 Experiment

The measurement method for the Lorentz angle is via cluster size measurements. In the absence of a magnetic field, the minimum average cluster size should occur at an

incidence angle of zero degrees, when the track is perpendicular to the wafer surface. When a magnetic field is applied, the Lorentz force will cause the moving charge (both electrons and holes) to deviate by an angle equal to the Lorentz angle. Thus the position of the minimum of the average cluster size will shift. In order to find the Lorentz angle, the sensor is rotated to change incidence angle and find the angle corresponding to the minimum cluster size, as seen in Figure (5).

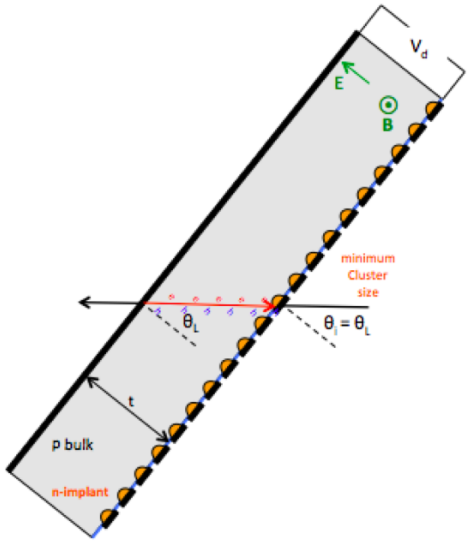

Figure 5: Schematic picture that represents how the minimum cluster size happens at the Lorentz angle in the presence of a magnetic field.

2.3 Experiment setup

The setup of the Lorentz angle measurement [7] consists of the following:

- **Beam** Electrons from DESY II test beam facility (1-5 GeV).
- **Superconducting solenoid** Generates a magnetic field up to 1T.
- **Beam Telescope** EUDET beam telescope is used. Its purpose is to find the incidence angle of the particle on the sensor.
- **Device Under Test (DUT)** It consists of the two ATLAS miniature sensors attached to the Alibava Daughter Board (see next section) and a cooling system. The sensors are cooled down to ~ -25 °C to prevent annealing of the irradiated samples and to avoid leakage current.

3 Analysis of the Pedestal signal in the Alibava Readout System

3.1 The Alibava Readout System

The Alibava readout system [8] is dedicated to the research of strip sensors. The readout system consists of two boards: The mother board and the daughter board. The primary analogue readout system is placed on the daughter board. It consists mainly of two Beetle readout chips that are operated in analogue readout mode. The Beetle chip is used for the readout and amplification of the collected charge from the individual sensor strips. It has 128 channels with an amplifier and a shaper. The amplified and shaped signal pulse is sampled into an analogue pipeline with the LHC bunch-crossing frequency of 40MHz. The analogue data is measured in analogue-digital-counts (ADC). The data that is brought off the chip is transferred via a flat cable to the mother board, where it is processed and digitalised. The mother board communicates with the data acquisition software on a computer.

3.2 Analysis of the Pedestal

The experiment took place in the period of time 2013 and 2014. During the running of the experiment we were allowed to turn off the beam and analyse the signal when the sensor was not exposed to any electron beam. In these cases, despite the fact that there are no particles passing through the sensor, the electrical signal that we get is not zero. There is a background signal due to our electronic devices. The aim of this project was to analyse that signal, named pedestal, and its fluctuation around the mean value which is the noise. These two magnitudes are of basic importance to make further analysis on the Lorentz angle measurement. The dependence of pedestal and noise on temperature and magnetic field are studied in this project.

3.2.1 Method and Procedure

The Alibava readout system provides us with an analog signal in ADCs, which is proportional to the collected charge. The histogram of the reading that we get from one channel (i.e strip) fits to a normal distribution. The mean value is the pedestal and its standard deviation is the noise. An example is shown in Figure (6). The plots shown in this section are obtained from a non-irradiated ATLAS miniature sensor connected to one chip in a daughter board in zero magnetic field.
This calculation can be done for all the channels and we end up having the mean pedestal and noise for each channel, as seen in Figure (7).
Now, by subtracting the mean pedestal of each channel from the reading in a specific event we may still see that all channels have similar noise. This is what we call common mode noise. We calculate the mean value of common mode noise and subtract it from the reading. If we make the histogram of the common mode noise we find a normal

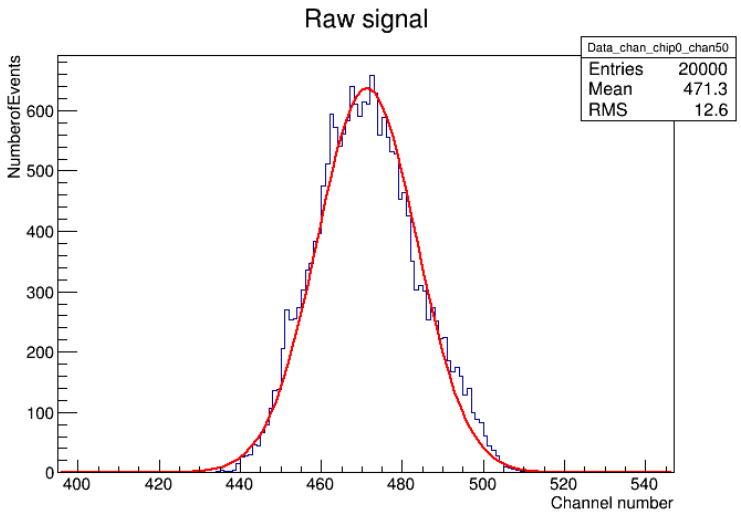

Figure 6: Histogram of the readings in a specific run and specific channel. The pedestal corresponds to the mean value of the fitted normal distribution. The noise is the standard deviation of the distribution.

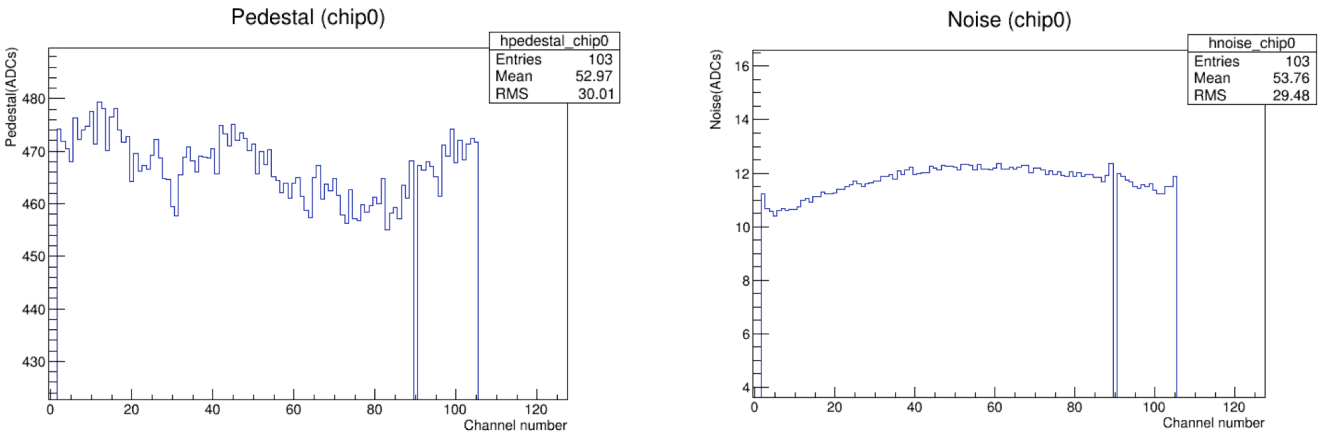

Figure 7: Plots of the mean pedestal and noise of each channel.

distribution centred around zero as shown in Figure (8). After subtracting the pedestal and common mode noise from the reading we can recalculate the pedestal and noise of each channel. We see in Figure (9) how the recalculated signal fits to a narrower normal distribution. The mean and the standard deviation of the distribution are the pedestal and noise after common mode correction. A comparison plot between pedestal and noise before and after common mode correction is shown in Figures (10) and (11).

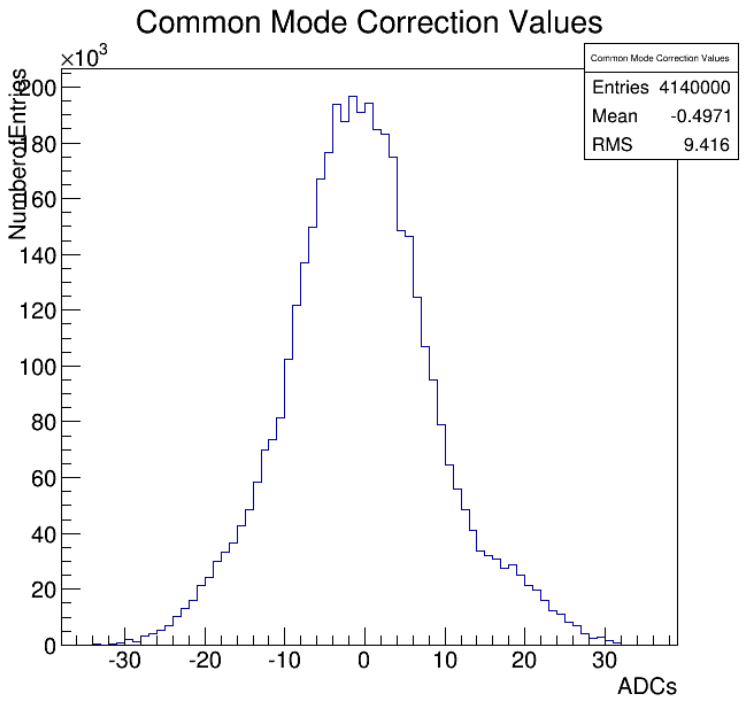

Figure 8: Histogram of the common mode noise for one run.

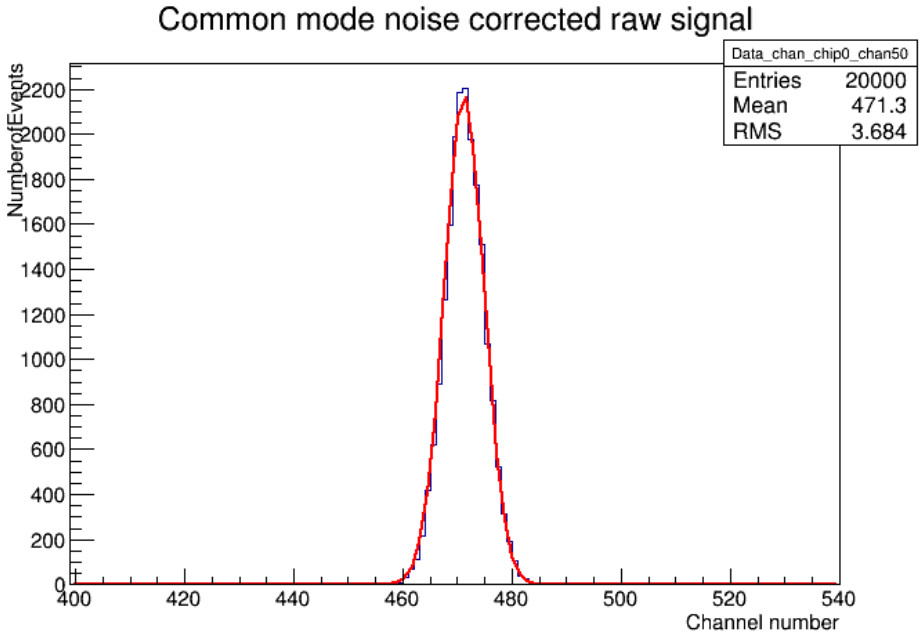

Figure 9: Histogram of the readings in a specific run and specific channel. The pedestal corresponds to the mean value of the fitted normal distribution. The noise is the standard deviation of the distribution.

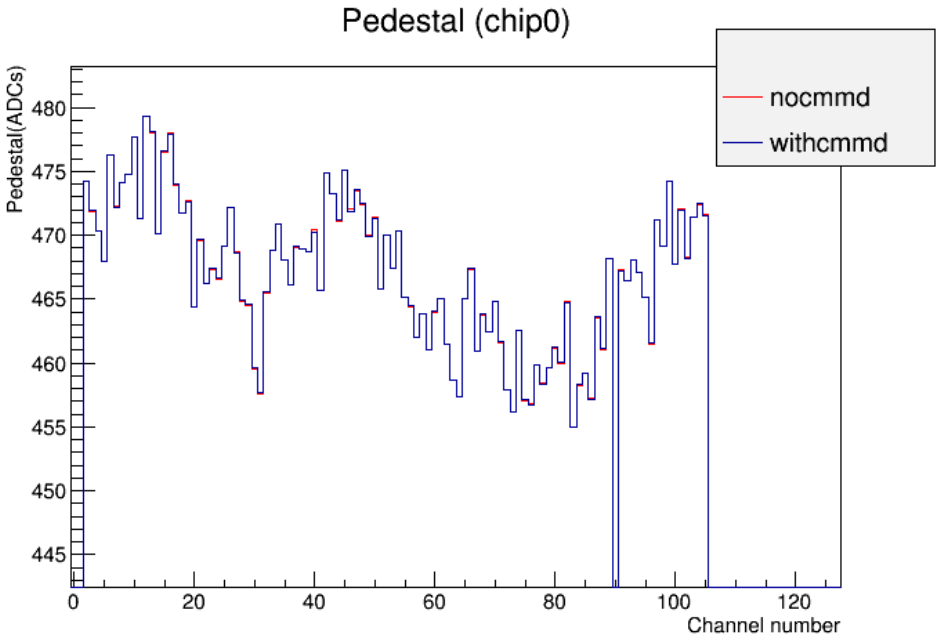

Figure 10: Pedestal comparison before and after applying common mode correction. Red and blue lines show the pedestal before and after common mode noise correction respectively.

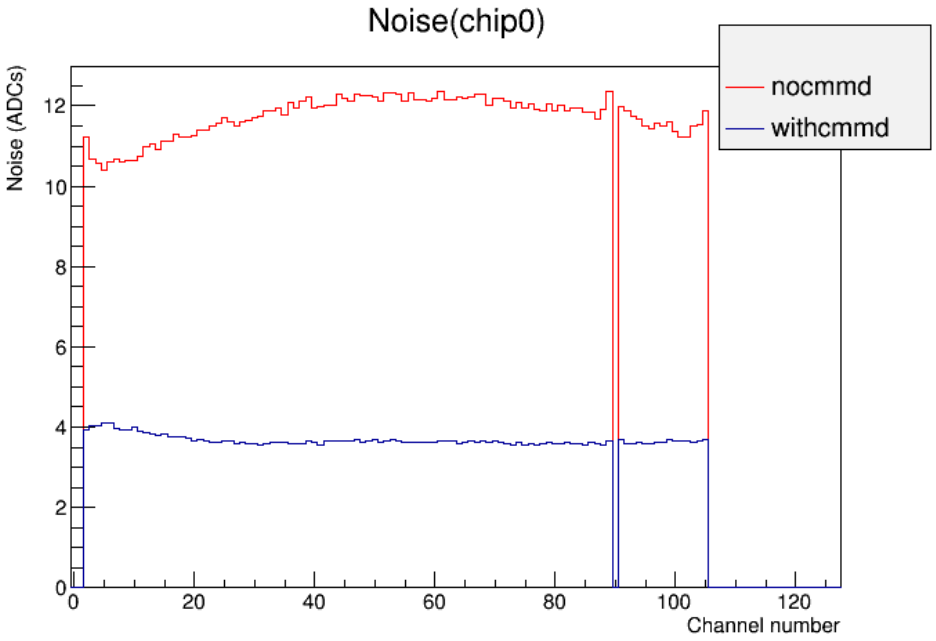

Figure 11: Noise comparison before and after applying common mode correction. Red and blue lines show the noise before and after common mode noise correction respectively.

4 Results

The results of the analysis are shown in this section. In the first part of the analysis we compare the pedestal and noise that we get for a range of temperatures that don't exceed 1 degree Celcius. This is done independently for non-irradiated, irradiated and annealed sensors. In the second part we analyse this dependence with data taken at different magnetic fields for a non-irradiated sensor. Note that we have two independent temperatures: chipT and sensorT, corresponding to the chip and sensor temperatures and measured in degrees Celcious. In both cases the temperature differences don't exceed 1 degree. We only show the results for one of the chips, named chip 0. For each analysis the plots show the absolute values in ADCs of pedestal and noise on the left and the relative difference in percentage on the right. For computing the relative difference in percentage of pedestal and noise we always take the first run as the reference value.

4.1 Pedestal and noise dependence on small change in temperature and zero magnetic field

In this section we give the results of pedestal and noise dependence on a temperature change of less than 1 degree Celcious. We studied three cases: non-irradiated, irradiated and annealed. In all of them we keep the magnetic field zero.

4.1.1 Non-Irradiated sensor

In Figure (12) we show the pedestal and noise for 3 different runs at B=0. All of them are from a non-irradiated sensor. A small change in pedestal between runs is observed. The mean value of the relative change for the second run is 0.12% while for the third is 0.14%, see Table (1). On the other hand the noise is small compared to the pedestal. Its variation throughout different runs always fluctuates around the zero value and doesn't exceed $\sim 2\%$.

Table 1: Relative difference of pedestal values on non-irradiated sensor at $B = 0$.

Relative difference (%)	ΔT sensor (°C)	ΔT chip (°C)
0.12%	0.32	0.49
0.14%	0.24	0.37

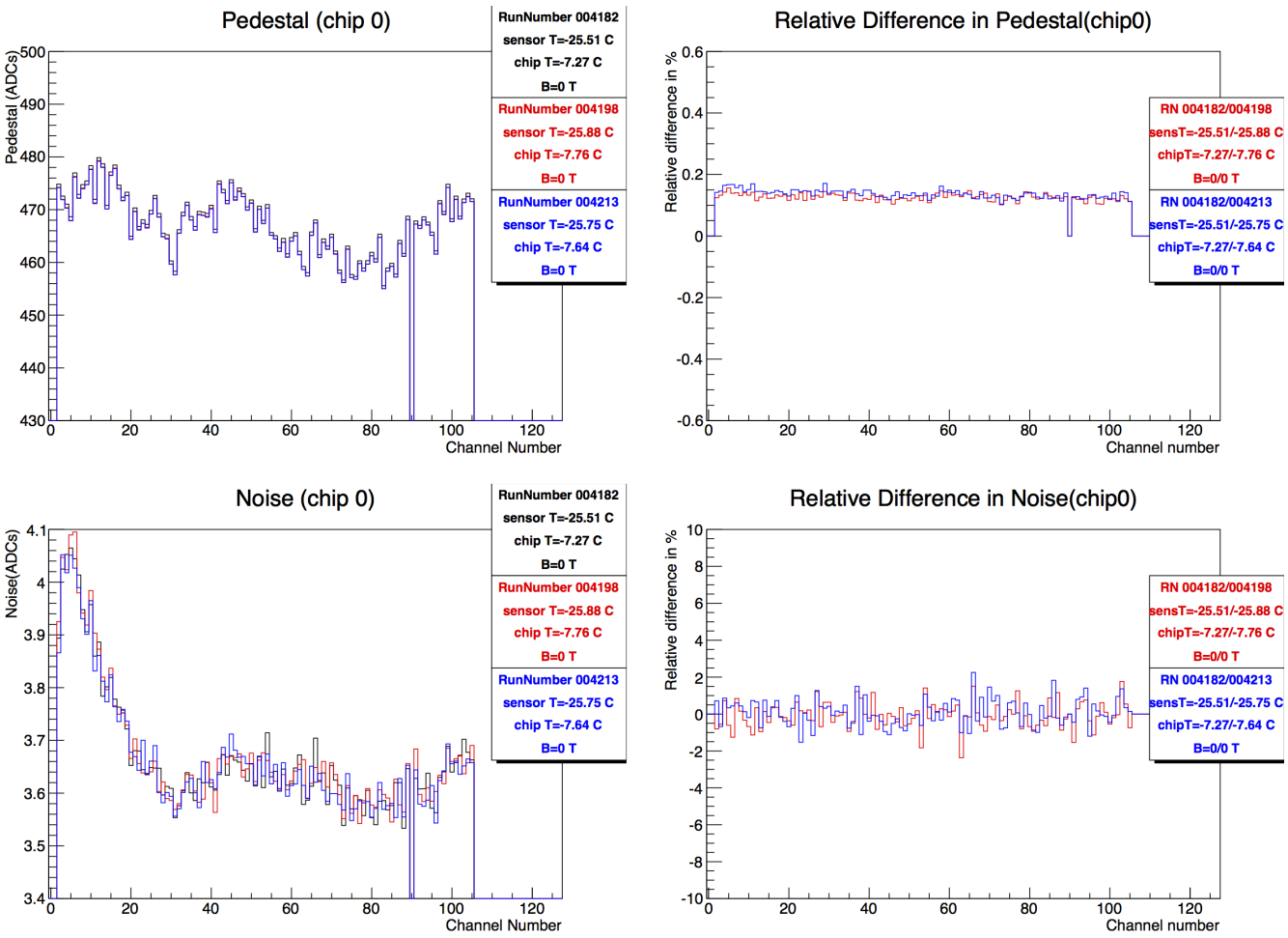

Figure 12: Pedestal and noise signal from a non-irradiated sample measured in ADCs for different runs. All of them from chip 0.

4.1.2 Irradiated Sensor

In Figure (13) we show the pedestal and noise for 4 different runs at B=0. All of them are from an irradiated sensor at a level of $2\times10^{14}(1MeVn_{eq})/\text{cm}^2$. Again, a slightly constant change in pedestal between runs is observed. The relative difference in percentage fits also to a constant. The mean values of the relative difference, in the same order as in the plot legend, are: 0.30%, 0.32% and 0.30%, see Table (2). On the other hand the noise variation always fluctuates around the zero and doesn't exceed $\sim 3\%$.

Table 2: Relative difference of pedestal values on irradiated sensor at $B = 0$.

Relative difference (%)	ΔT sensor (°C)	ΔT chip (°C)
0.30%	0.11	0.23
0.32%	0.16	0.50
0.30%	0.18	0.35

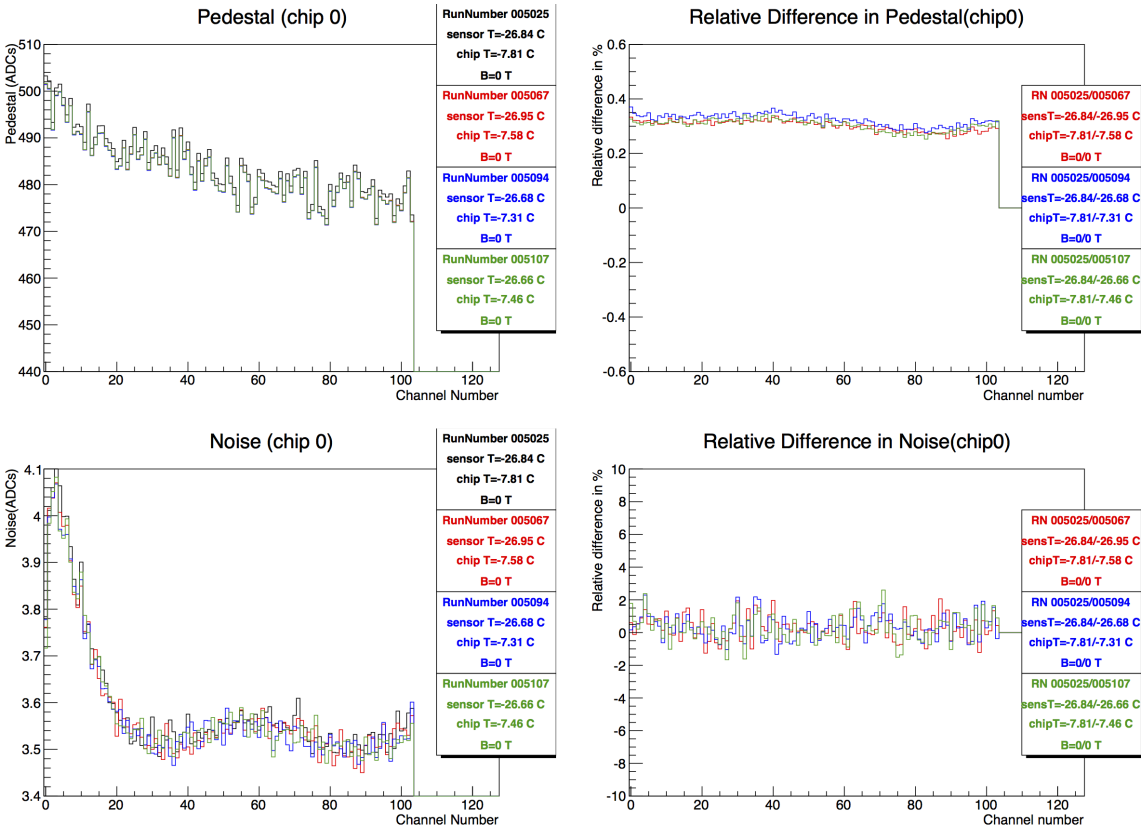

Figure 13: Pedestal and noise signal from an irradiated sample measured in ADCs for different runs. All of them from chip 0.

4.1.3 Annealed Sensor

In Figure (14) we show the pedestal and noise for 4 different runs at B=0. This is the same sensor used in section 4.1.2 but after annealing at 60 °C for 80min. We found again a small change in pedestal between runs. The mean values of the relative difference, in the same order as in the plot legend, are: -0.04% and -0.03%, see Table (3). On the other hand the noise variation always fluctuates around the zero value as before without exceeding $\sim 3\%$.

Table 3: Relative difference of pedestal values on annealed sensor at $B = 0$.

Relative difference (%)	ΔT sensor (°C)	ΔT chip (°C)
-0.04%	0.24	0.26
-0.03%	0.17	0.10

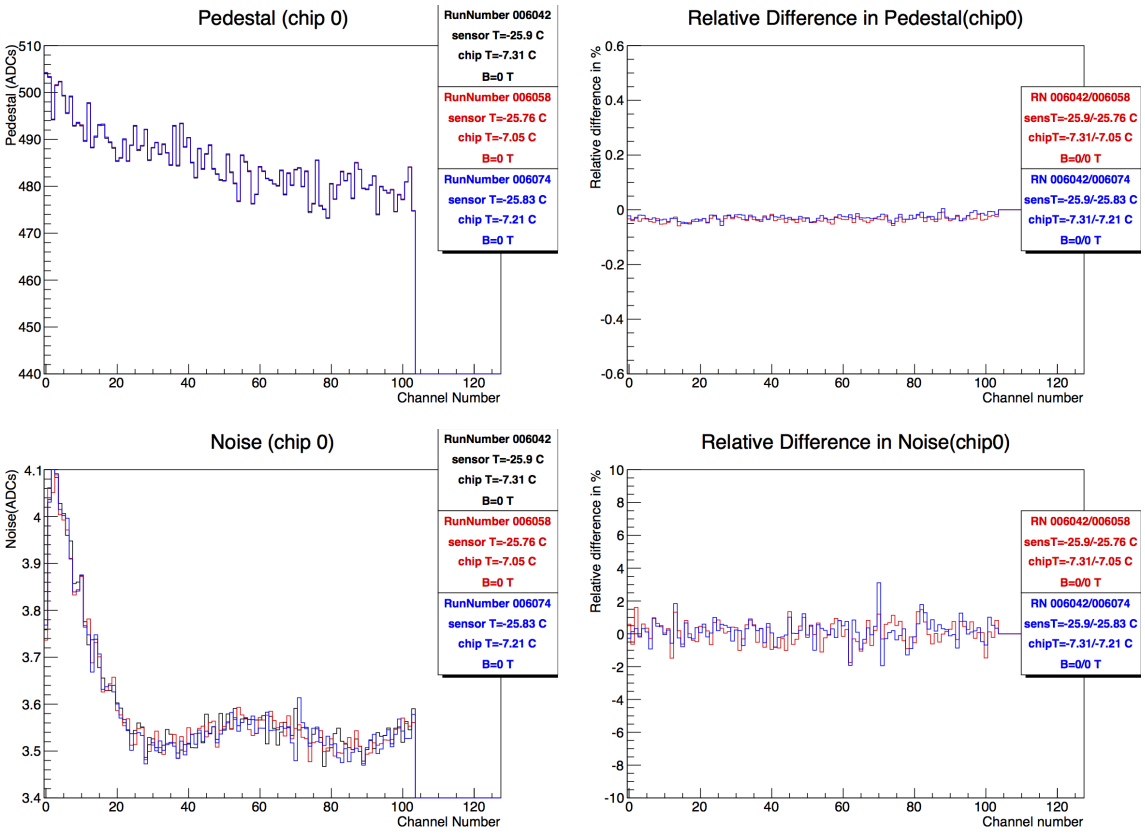

Figure 14: Pedestal and noise signal from the annealed sample measured in ADCs for different runs. All of them from chip 0.

4.2 Pedestal and noise dependence on magnetic field

Finally, as shown in Figure (15), we check if the change in pedestal and noise is affected by a change in magnetic field. All the runs that are shown are from a non-irradiated sensor. We show runs of magnetic field: 0, 0.5, 0.75 and 1T. The mean values of the relative difference, in the same order as in the plot legend, are: 0.28%, 0.23% and 0.28%, see Table (4). The noise variation always fluctuates around the zero without exceeding $\sim 2\%$.

Table 4: Relative difference of pedestal values on non-irradiated sensor for different magnetic fields.

Relative difference (%)	ΔT sensor (°C)	ΔT chip (°C)	B (Tesla)
0.28%	0.08	0.05	0.5
0.23%	0.10	0.02	0.75
0.28%	0.14	0.14	1

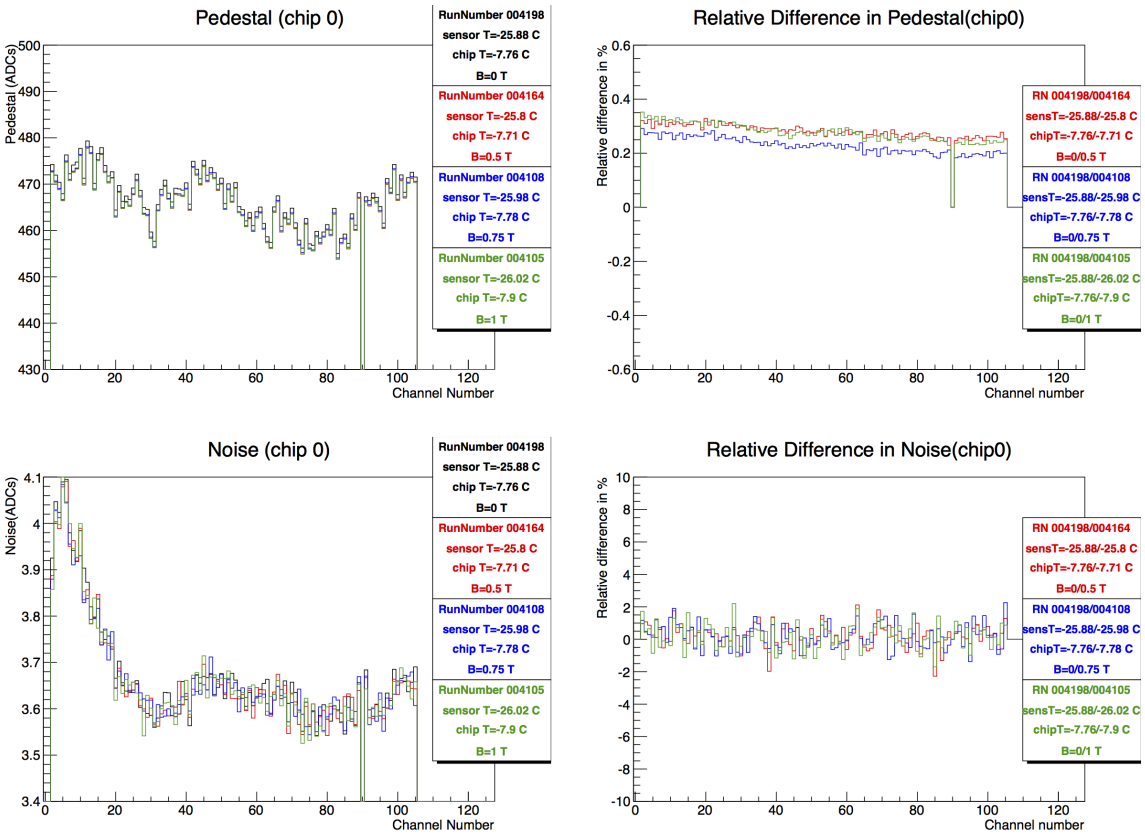

Figure 15: Pedestal Signal measured in ADCs for different runs. All of them from chip 0.

5 Conclusions

During the Lorentz angle measurement experiment part of the readout system is exposed to changes of temperature, irradiation and magnetic field. We wanted to know how this changes affect the pedestal and noise of our Alibava readout system. The aim of this project was to study the dependence of pedestal and noise values of the Alibava readout system on temperature and magnetic field. The effect of small temperature differences is analysed on non-irradiated, irradiated and annealed sensors. We showed that the relative difference in pedestal doesn't exceed $\sim 1\%$ when temperature differences are below 1 degree for non-irradiated, irradiated and annealed, nor for different magnetic field in a non-irradiated sample. Nevertheless its regular change is demanding of an interpretation. Where the offset comes from is not clear yet and it needs a further study. Finally, for all the runs checked so far with the same setup parameters and temperature differences below 1 degree we found that the differences in noise are not significant.

6 Acknowledgements

I would like to thank Eda Yildirim for her constant support and help during the preparation and writing of this project. I really appreciate her patience, kindness and advice at all times. I would also like to thank the ATLAS group for providing me the opportunity to join their work during this program. Finally I want to thank all the people that have helped me at some point during my stay at DESY. Because of them I will always remember this experience with sincere gratitude. Thank you.

References

[1] David Griffiths , *Introduction to Elementary Particles*, 2008 WILEY-VCH.

[2] ATLAS Detector, *atlas.ch/detector.html*, August 2014.

[3] ATLAS Inner Detector, *atlas.ch/inner-detector.html*, August 2014.

[4] ATLAS Collaboration, *ATLAS Letter of Intent: Phase II Upgrade*, CERN-2012-022 LHCC-I-023, (December 2012).

[5] Ruth Jacobs, *Development of a setup for the characterisation of silicon strip sensors using the ALiBaVa readout system and measurements on proton-irradiated samples*, CERN, Summer Student Report, (2013).

[6] T.Lari, *Lorentz Angle variation with electric field for ATLAS silicon detectors*, ATL-INDET-2001-004.

[7] Eda Yildirim, DESY *Lorentz Angle Measurement*, Bucharest, RD50 Workshop, June 12, 2014.

[8] Ricardo Marco-Hernández and ALIBAVA COLLABORATION. *A Portable Readout System for Microstrip Silicon Sensors (ALIBAVA)*, IEEE Transactions on Nuclear Science, Vol.56, No.3, June 2009.